PTEP

Prog. Theor. Exp. Phys. **2015**, 111A01 (11 pages)
DOI: 10.1093/ptep/ptv152

Letter

Hamilton dynamics for Lefschetz-thimble integration akin to the complex Langevin method

Kenji Fukushima[1] and Yuya Tanizaki[1,2*]

[1]*Department of Physics, The University of Tokyo, 7-3-1 Hongo, Bunkyo-ku, Tokyo 113-0033, Japan*
[2]*Theoretical Research Division, Nishina Center, RIKEN, Wako 351-0198, Japan*
*E-mail: yuya.tanizaki@riken.jp

Received July 31, 2015; Revised September 11, 2015; Accepted September 17, 2015; Published November 16, 2015

The Lefschetz-thimble method, i.e., integration along the steepest descent cycles, is a way to avoid the sign problem by complexifying the theory. We discuss that such steepest descent cycles can be identified as ground-state wave functions of a supersymmetric Hamilton dynamics, which is described with a framework akin to the complex Langevin method. We numerically construct the wave functions on a grid using a toy model and confirm their well-localized behavior.

Subject Index A22, A24, B15

1. *Introduction* A first-principles approach to solving the theory is the ultimate goal of theoretical investigations. The quantum Monte Carlo simulation for the functional integral is a powerful ab initio technique to reveal the nonperturbative features of various physical systems. Successful applications include the lattice QCD (quantum chromodynamics) simulation, the lattice Hubbard model, the path-integral representation of spin systems, etc.

The Monte Carlo algorithm is based on importance sampling, so it is required that the integrand should be positive semidefinite, i.e., $e^S \geq 0$, where S is the classical action. This positivity condition is often violated in systems of interest to us and then we can no longer rely on Monte Carlo simulations [1,2]. In QCD, a finite baryon or quark density introduces a mixture of Hermitian and anti-Hermitian terms in the action, and then e^S acquires a complex phase. In the repulsive Hubbard model away from half-filling or, generally, in fermionic systems with spin imbalance, the sign of the integrand may fluctuate. It is also a notorious problem of the complex phase that appears from the Berry curvature in the path-integral representation of spin systems; this phase cannot be removed for frustrated situations such as the XY model on the Kagomé lattice.

Moreover, to approach real-time quantum phenomena, e^S is an oscillating function by definition and the sign problem is unavoidable. Although the Monte Carlo simulation is useful to compute physical observables in equilibrium in the imaginary-time formalism, analytical continuation is necessary to access real-time information. In general, however, analytical continuation is quite a costly procedure, and some additional information on the system, such as the pole and the branch-cut structures, would be necessary.

Many ideas have been proposed so far to overcome the sign problem; unfortunately, the applicability of each method is severely limited. Recently, new techniques to complexify the theory have been

attracting more and more theoretical interest; these techniques include the path integral on Lefschetz thimbles [3–14] and the complex Langevin approach [15–21]. Except for several formal arguments, theoretical foundations for the complex Langevin method are not fully established, and not much is known about its reliability [16–18]. In the context of real-time quantum systems, the numerical simulation works for some initial density matrices [19,20]; however, it was recently reported in Ref. [21] that the real-time anharmonic oscillator at zero temperature converges to a wrong answer with unphysical width.

In contrast, the Lefschetz-thimble method has a solid mathematical foundation at least for finitely multiple integrals [3–5]; however, its practical applicability is still in the developing stage. This method decomposes the original integration cycle into several steepest descent ones, called Lefschetz thimbles, using complexified field variables. Picking up a single Lefschetz thimble, one can employ importance sampling [6–8] and avoid the sign problem since the oscillatory factor in e^S totally disappears on each Lefschetz thimble. On the other hand, 0D model studies have exemplified the importance of structures of multiple Lefschetz thimbles [10–13]. For further applications, it is necessary to deepen our understanding on more aspects of Lefschetz thimbles.

The purpose of this letter is to shed new light on the Lefschetz-thimble method in a form of Hamilton dynamics, which was first elucidated in Ref. [5]. In this reformulation, the Lefschetz thimbles can be identified as ground-state wave functions of a supersymmetric topological quantum system. After reviewing this modified Lefschetz-thimble method, for a quartic potential problem at zero dimensions, we solve the Hamilton dynamics concretely to find the corresponding wave functions. Based on our analytical and numerical observations, we discuss the advantages of this reformulation for the numerical computation.

2. *Lefschetz thimble and SUSY quantum mechanics*

Let us consider an N-dimensional real integral as a "quantum field theory" defined by a (complex) classical action $S(x)$. In this theory, our goal is to compute an expectation value of an "observable" $\mathcal{O}(x)$ defined by

$$\langle \mathcal{O} \rangle = \mathcal{N} \int_{-\infty}^{\infty} d^N x \; e^{S(x)} \, \mathcal{O}(x), \tag{1}$$

where $x = \left(x^{(1)}, x^{(2)}, \ldots, x^{(N)}\right) \in \mathbb{R}^N$ and the normalization $\mathcal{N}$ is chosen such that $\langle 1 \rangle = 1$. The starting point in our discussion is to reformulate this theory in an equivalent and more treatable way using a complexified representation:

$$\langle \mathcal{O} \rangle = \int d^N z \, d^N \bar{z} \; P(z, \bar{z}) \, \mathcal{O}(z). \tag{2}$$

Here $z^{(i)} = x_1^{(i)} + i x_2^{(i)}$ and $\bar{z}^{(i)} = x_1^{(i)} - i x_2^{(i)}$, with $x_1^{(i)}, x_2^{(i)} \in \mathbb{R}$, and $\int dz d\bar{z}$ represents the integration over the whole complex plane; i.e., $\int_{-\infty}^{\infty} dx_1 \int_{-\infty}^{\infty} dx_2$. The choice of the generalized weight function $P(z, \bar{z})$ may not be unique. Indeed, a trivial example is $P(z, \bar{z}) = \mathcal{N} e^{S(z)} \prod_i \delta\left(z^{(i)} - \bar{z}^{(i)}\right)$. At the cost of complexifying the variables, nevertheless, it is often the case that $P(z, \bar{z})$ could be endowed with more desirable properties for analytical and numerical computation than the original $e^{S(x)}$.

A clear criterion to simplify the integral is to find $P(z, \bar{z})$ such that the phase oscillation can be suppressed along integration paths as much as possible, while, in the complex Langevin method, $P(z, \bar{z})$ is optimized to become a real probability. To suppress the phase oscillation, let us pick up a saddle point z_σ satisfying $S'(z_\sigma) = 0$. The steepest descent cycle or the Lefschetz thimble $\mathcal{J}_\sigma$ of the

saddle point z_σ is defined with a fictitious time t as

$$\mathcal{J}_\sigma = \left\{ z(0) = x_1(0) + i x_2(0) \,\middle|\, \frac{dx_j^{(i)}(t)}{dt} = -\frac{\partial \mathrm{Re}\, S}{\partial x_j^{(i)}},\ \lim_{t\to-\infty}(x_1(t)+ix_2(t)) = z_\sigma \right\}. \tag{3}$$

This is a multi-dimensional generalization of the steepest descent path in complex analysis, which we will refer to as the *downward* path. The original integration path on the real axis in Eq. (1) can be deformed as a sum of contributions on $\mathcal{J}_\sigma$ weighted with an integer m_σ; i.e., $\int_{\mathbb{R}^N} d^N x = \sum_\sigma m_\sigma \int_{\mathcal{J}_\sigma} d^N z$. In mathematics it is established how to determine m_σ from the intersection pattern between the steepest ascent (*upward*) path from z_σ and the original integration path [3–5]. It is important to note that Im S is a constant on each Lefschetz thimble for the application to the sign problem [6,8].

In the following, let us restrict ourselves to $N = 1$ for simplicity, because the generalization is straightforward. So far, the Lefschetz thimble is constructed as a line; let us find a 2D smooth distribution $P(z, \bar{z})$ according to Ref. [5]. For that purpose, we define the "delta-functional one-form" $\delta(\mathcal{J}_\sigma)$ supported on the Lefschetz thimble so that

$$\int_{\mathcal{J}_\sigma} \mathcal{O}(z) e^{S(z)} dz = \int_{\mathbb{C}} \delta(\mathcal{J}_\sigma) \wedge \mathcal{O}(z) e^{S(z)} dz. \tag{4}$$

For instance, $\delta(\mathbb{R}) = \delta(y)dy$. Such delta-functional forms $\delta(\mathcal{J}_\sigma)$ (on a Kähler manifold) have a path-integral expression from the supersymmetric quantum mechanics [22–24] (see also Sects. 2.8 and 4 of Ref. [5] for more details in this context). Integration (4) can be represented as

$$\begin{aligned}\langle \mathcal{O} \rangle = \mathcal{N} \int \mathcal{D}[x, p, \pi, \psi]\ \exp\left[i \int_{-\infty}^{0} dt p_i \left(\frac{dx_i}{dt} + \frac{\partial \mathrm{Re} S}{\partial x_i} \right) \right] \\ \times \exp\left[- \int_{-\infty}^{0} dt\, \pi_i \left(\frac{d}{dt}\delta_{ij} + \frac{\partial^2 \mathrm{Re}\, S}{\partial x_i \partial x_j} \right) \psi_j \right] \mathcal{O}(z(0))\, e^{S(z(0))}\, (\psi_1 + i\psi_2)(0).\end{aligned} \tag{5}$$

Here x, p are bosonic fields, π, ψ are fermionic ghost fields, and $z(t) \to z_\sigma$ as $t \to -\infty$. We should note that an integration in terms of z is promoted to the path integral on $z(t)$ for $t \le 0$, while the observable and the weight $\mathcal{O}(z(0)) \exp S(z(0))$ are functions of $z(0)$ only. Let us outline how these two expressions (4) and (5) are equivalent [5,22–24]. We first integrate out $p(t)$ to get the Dirac delta function:

$$\int \mathcal{D}p\, \exp\left[i \int_{-\infty}^{0} dt p_i \left(\frac{dx_i}{dt} + \frac{\partial \mathrm{Re} S}{\partial x_i} \right) \right] = \delta\left(\frac{dx_i}{dt} + \frac{\partial \mathrm{Re} S}{\partial x_i} \right). \tag{6}$$

This delta function constrains the path integral on $x(t)$ to a gradient-flow line defining Lefschetz thimbles. Since $z(-\infty) \to z_\sigma$, this path integral for $t < 0$ gives a delta-functional support on $\mathcal{J}_\sigma$. However, the delta function produces an unwanted determinant factor. As is well known, the path integral on ghost fields $\pi(t)$, $\psi(t)$ for $t < 0$ can eliminate that factor as

$$\int \mathcal{D}\pi\, \mathcal{D}\psi\, \exp\left[- \int_{-\infty}^{0} dt \pi_i \left(\frac{d}{dt}\delta_{ij} + \frac{\partial^2 \mathrm{Re}\, S}{\partial x_i \partial x_j} \right) \psi_j \right] = \mathrm{Det}\left(\frac{d}{dt}\delta_{ij} + \frac{\partial^2 \mathrm{Re}\, S}{\partial x_i \partial x_j} \right). \tag{7}$$

Now, we obtain an integration over surface variables $x(0)$, $\psi(0)$, and denote them by x, ψ. Locally, the Lefschetz thimble $\mathcal{J}_\sigma$ can be expressed as zeros of a certain function f; then we can find that the path integral (5) eventually gives

$$\int d^2x d^2\psi\, \delta(f)\, \frac{\partial f}{\partial x_i}\psi_i \wedge \mathcal{O}(z)\, e^{S(z)}\, (\psi_1 + i\psi_2) = \int \delta(f(x)) df(x) \wedge \mathcal{O}(z)\, e^{S(z)}\, dz, \tag{8}$$

which is nothing but the local expression of the original integration (4). Going back to (5), this shows that the so-called residual sign problem comes from the fermionic surface term $\psi_1(0) + i\psi_2(0)$ because one can identify $\psi_i(0) = dx_i$ as above.

Importantly, with these added fields, p_i, π_i, ψ_i, the action is BRST exact under a transformation: $\hat{\delta} x_i = \psi_i, \hat{\delta}\psi_i = 0, \hat{\delta}\pi_i = -ip_i, \hat{\delta} p_i = 0$. By definition, the nilpotency $\hat{\delta}^2 = 0$ is obvious. Thanks to the boundary fermionic operator in (5), the surface term is BRST closed so long as the observables are holomorphic. This makes a sharp contrast to the complex Langevin method, which could also acquire BRST symmetry, but this symmetry is violated by the surface term. Because of the BRST symmetry, we can add any BRST-exact terms without changing the original integral, and it is useful to insert $\frac{\varepsilon_i}{2}\int dt\, p_i^2$. In summary, the effective Lagrangian that describes the fictitious time evolution is given by the following topological theory:

$$\begin{aligned} L_{\text{eff}} &= -\frac{\varepsilon_i}{2} p_i^2 + i p_i \left(\frac{dx_i}{dt} + \frac{\partial \text{Re} S}{\partial x_i} \right) + \pi_i \left(\frac{d}{dt}\delta_{ij} + \frac{\partial^2 \text{Re} S}{\partial x_i \partial x_j} \right) \psi_j \\ &= -\hat{\delta} \left\{ \pi_i \left(i\frac{\varepsilon_i}{2} p_i + \frac{dx_i}{dt} + \frac{\partial \text{Re} S}{\partial x_i} \right) \right\}, \end{aligned} \tag{9}$$

which is nothing but a Legendre transform of an effective Hamiltonian:

$$H_{\text{eff}} = \sum_i \left[\frac{\varepsilon_i}{2} \hat{p}_i^2 - \frac{i}{2} \left(\frac{\partial \text{Re} S}{\partial x_i} \hat{p}_i + \hat{p}_i \frac{\partial \text{Re} S}{\partial x_i} \right) \right] - \sum_{i,j} \frac{1}{2} \frac{\partial^2 \text{Re} S}{\partial x_i \partial x_j} [\hat{\pi}_i, \hat{\psi}_j] \tag{10}$$

with $[x_i, \hat{p}_j] = i\delta_{ij}$ and $\{\hat{\pi}_i, \hat{\psi}_j\} = \delta_{ij}$. The fermion number $F = \hat{\pi}_1\hat{\psi}_1 + \hat{\pi}_2\hat{\psi}_2$ is a conserved quantity of this Hamiltonian. After the time evolution from $t = -\infty$, only the ground state with the lowest-energy eigenvalue remains, so that the generalized weight is given by $P(z, \bar{z}) dz\, d\bar{z} = \Psi(z, \bar{z}) \wedge e^{S(z)} dz$, where $\Psi(z, \bar{z})$ is the ground-state wave function and converges to $\delta(\mathcal{J}_\sigma)$ in the limit $\varepsilon_i \to +0$. Note that the weight factor $\exp S(z)$ is necessary in this formula, since the wave function designates only the integration cycle $\mathcal{J}_\sigma$. We can further simplify this Hamilton problem by choosing $\varepsilon = \varepsilon_1 = \varepsilon_2$. Performing the conjugate transformation $\Psi = e^{-\text{Re}\, S/\varepsilon} \Psi'$, the first derivative terms are eliminated as

$$H'_{\text{eff}} = \sum_i \left[\frac{\varepsilon}{2} \hat{p}_i^2 + \frac{1}{2\varepsilon} \left(\frac{\partial \text{Re} S}{\partial x_i} \right)^2 \right] - \sum_{i,j} \frac{1}{2} \frac{\partial^2 \text{Re} S}{\partial x_i \partial x_j} [\hat{\pi}_i, \hat{\psi}_j]. \tag{11}$$

This describes supersymmetric quantum mechanics with the superpotential $\text{Re} S$ [5].

Before applying this method to an interacting model, let us convince ourselves of its perturbative correctness. For this purpose, we consider the simple Gaussian case:

$$S_0(x) = -\frac{\omega}{2} x^2, \tag{12}$$

where $x \in \mathbb{R}$ is a one-component variable and $\omega \in \mathbb{C}$. One can regard this Gaussian integral as an elementary building block of perturbative quantum field theory; in a noninteracting theory of the scalar field ϕ, the action is decomposed into $-\frac{1}{2}[\Gamma - i(k^2 - m^2)]\phi(-k)\phi(k)$ for each Fourier mode. In this case, we immediately find that the bosonic wave function should be the ground state of a harmonic oscillator with the ground-state energy $|\omega|$. The fermionic ground-state energy $-|\omega|$ cancels the bosonic energy thanks to supersymmetry. As a result, unoccupied fermions point in the direction of the Lefschetz thimble; i.e., the supersymmetric vacuum belongs to the $F = 1$ sector. Let us see this in the simplest example, $\omega \in \mathbb{R}$ and $\omega > 0$. The fermionic part of the Hamiltonian is $\frac{\omega}{2}\left(\left[\hat{\pi}_1, \hat{\psi}_1\right] - \left[\hat{\pi}_2, \hat{\psi}_2\right]\right)$, and thus the 1 and 2 fermions are unoccupied and occupied, respectively. This leads to the fermionic ground-state energy $-\omega$, which cancels the bosonic ground-state energy ω. Therefore, the unoccupied fermion is tangent to the Lefschetz thimble $\mathcal{J} = \mathbb{R}$.

The final result of $P_0(z, \bar{z})$ for $\omega \in \mathbb{C}$ together with $e^S \cdot e^{-\frac{1}{\varepsilon}\mathrm{Re}S}$ is

$$P_0(z, \bar{z}) = \mathcal{N}\exp\left[-\frac{|\omega|}{2\varepsilon}z\bar{z} + \frac{1}{4\varepsilon}\left(\omega z^2 + \bar{\omega}\bar{z}^2\right) - \frac{\omega}{2}z^2\right], \tag{13}$$

which reproduces the original integral (1) with the action (12). To see this for a polynomial $\mathcal{O}(x)$, it is sufficient to require $\langle z^2 \rangle = 1/\omega$, which is nothing but the free propagator and can be explicitly confirmed with Eq. (13). For the exponentially fast convergence of P_0, the parameter ε needs to be $0 \le \varepsilon < 2$. We here emphasize that the theory is equivalent to the original (1) for $0 \le \forall\varepsilon < 2$ and the conventional Lefschetz-thimble method is retrieved in the $\varepsilon \to 0$ limit. Actually, in this limit of $\varepsilon \to 0$, only a path of $2|\omega|z\bar{z} - \omega z^2 - \bar{\omega}\bar{z}^2$ $(\equiv\{2\mathrm{Im}(\sqrt{\omega}z)\}^2) = 0$ contributes, which is nothing but a condition to guarantee $\mathrm{Im}\, S_0(z) = 0$ on the Lefschetz thimble. At finite ε, this restriction is smeared and P_0 may have a distribution around $\mathcal{J}$ with a width of the order of ε where a complex phase arises in general. The nonpositivity of P_0 is a big difference between this Lefschetz-thimble approach and the complex Langevin method, in which the distribution must be semipositive definite.

In the model with quartic interaction, $S = -\frac{\omega}{2}z^2 - \frac{\lambda}{4}z^4$, the vacuum structure is drastically different from that of the Gaussian case (13). With $\lambda \neq 0$, there are three classical saddle points and the Morse index for each saddle point is 1. The Witten index is $\mathrm{tr}(-1)^F = -3$, and thus there are three supersymmetric vacua in this interacting model for any ε [25,26]. In the path-integral expression (5), we can distinguish these three vacua by specifying the boundary condition at $t = -\infty$, as we will discuss below in detail.

3. *Lefschetz thimbles at $\varepsilon \to 0$* We define our 0D model with the quartic interaction by

$$S(x) = -\frac{\omega}{2}x^2 - \frac{\lambda}{4}x^4, \tag{14}$$

and, hereafter, we will specifically choose the model parameters as

$$\omega = 1 - i = \sqrt{2}e^{-i\pi/4}, \quad \lambda = 1.5i. \tag{15}$$

This choice is motivated by the application to real-time problems. As we have already mentioned, $\mathrm{Re}\omega$ corresponds to the width Γ or ϵ in the $i\epsilon$ prescription, and $\mathrm{Im}\,\omega$ corresponds to $-(k^2 - m^2)$. Therefore, the parameters (15) represent a situation at $k^2 = m^2 + \Gamma$ in quantum field theory.

When ε is small enough, the Hamilton dynamics should become equivalent to the conventional formulation of the integral on the Lefschetz thimble, which means that $P(z, \bar{z})$ should have a

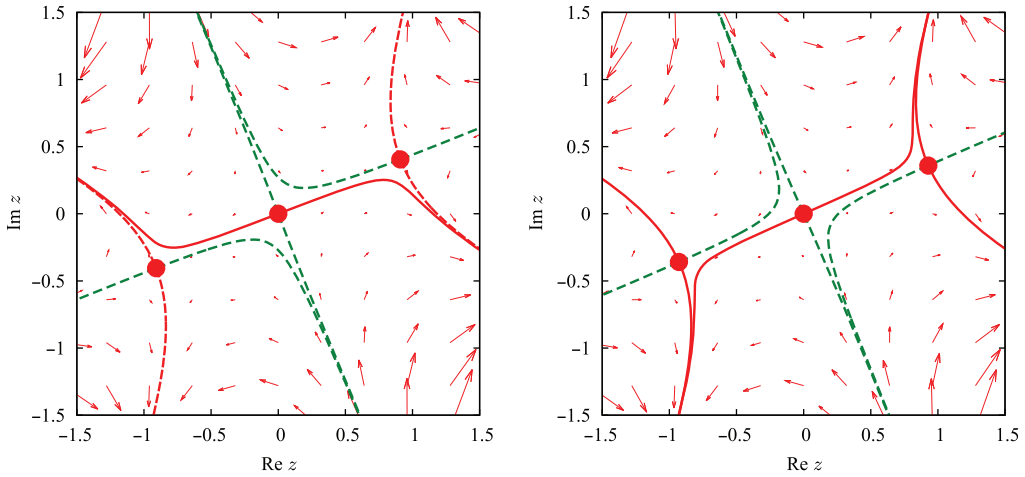

Fig. 1. Changes of the Lefschetz thimbles for $\omega = 1 - 0.9i$ (left) and $\omega = 1 - 1.1i$ (right) with $\lambda = 1.5i$ fixed. (Left) One of three thimbles contributes to the integral, as shown by the solid line, and two are to be dropped when $\omega = 1 - 0.9i$. (Right) All three thimbles contribute to the integral when $\omega = 1 - 1.1i$.

peak along the Lefschetz thimble only. This makes the analytic treatment very accessible, since we do not have to solve the quantum-mechanical problem in this 0D toy model. To identify the Lefschetz thimble, we should integrate the flow equation in Eq. (3) and find the upward and downward paths. We show the numerical results in Fig. 1 for parameters slightly changed from Eq. (15).

For our theory (14), three saddle points are located at $z_0 = 0$, $z_\pm = \pm\sqrt{-\omega/\lambda}$. The latter is, for our choice of parameters (15), $z_\pm = \pm(0.897 + 0.372i)$, and $S(z_\pm) = -1/3$. We can see that $\omega = 1 - i$ is a critical value at which the destinations of the downward flows from the saddle points change drastically, known as the Stokes phenomenon, as is clear from the two panels for $\omega = 1 - 0.9i$ (left) and $\omega = 1 - 1.1i$ (right) in Fig. 1. In general, we can show that the Stokes phenomenon occurs at $\mathrm{Im}\,(\omega^2/\lambda) = 0$, and, when λ is pure imaginary, this condition gives $\arg(\omega) = -\pi/4$. Importantly, not only the downward flows but also the upward flows change, and the intersection number of the original and upward paths changes accordingly [4,5]. In the case with $\omega = 1 - 0.9i$, only one upward path from z_0 crosses the real axis, as seen in the left panel of Fig. 1, and so the Lefschetz thimble going through z_0 contributes to the integral. In the case with $\omega = 1 - 1.1i$, on the other hand, three upward paths from z_0 and $z_\pm$ all cross the real axis, and all three Lefschetz thimbles contribute to the integral.

Keeping the potential application to real-time physics in mind, we need a deeper understanding of the Stokes phenomenon. In fact, it occurs at $k^2 = m^2 + \Gamma$ and so the thimble structure may fluctuate depending on the frequency k^0, while in Euclidean theory it never happens because $k^2 - m^2$ is always negative (except for an unstable potential with $m^2 < 0$). It should be an interesting future problem to clarify the treatment of the Stokes phenomenon in real-time systems [10].

For the same model with a different set of parameters, the Stokes phenomenon has been discussed in Refs. [27,28] and the probability distribution $P(z, \bar{z})$ in the complex Langevin method has been numerically computed. The important insight obtained there is that $P(z, \bar{z})$ in the complex Langevin method looks localized but has a power decay at large $|z|$, which causes a convergence problem. Hence, it would be an intriguing question to see how $P(z, \bar{z})$ in the modified Lefschetz-thimble method for $\varepsilon \neq 0$ should behave, especially at large $|z|$.

4. *Wave functions at finite ε* As an application of the modified Lefschetz-thimble method with a regulator ε, let us compute the wave function Ψ' for the $\varepsilon = \varepsilon_1 = \varepsilon_2$ case, from which $P(z, \bar{z})$ is to be constructed immediately. We can readily find the eigenstate in terms of ψ_i for the last term in the Hamiltonian (11). By restricting ourselves to the $F = 1$ sector, we can define the effective potential in the form of a 2×2 matrix-valued function that amounts to

$$V_{\text{eff}} = \frac{1}{2\varepsilon}\left[\left(\frac{\partial \text{Re}S}{\partial x_1}\right)^2 + \left(\frac{\partial \text{Re}S}{\partial x_2}\right)^2\right] - \begin{pmatrix} \partial^2 \text{Re}S/\partial x_1^2 & \partial^2 \text{Re}S/\partial x_1 \partial x_2 \\ \partial^2 \text{Re}S/\partial x_1 \partial x_2 & -\partial^2 \text{Re}S/\partial x_1^2 \end{pmatrix}, \tag{16}$$

and then the Hamiltonian is

$$H'_{\text{eff}} = -\frac{\varepsilon}{2}\left(\frac{\partial^2}{\partial x_1^2} + \frac{\partial^2}{\partial x_2^2}\right) + V_{\text{eff}}. \tag{17}$$

Let us solve the ground state of the above H'_{eff} at finite ε; we specifically adopt $\varepsilon = 1$ unless stated explicitly.

When we solve the Hamilton dynamics, we should set initial conditions to select proper Lefschetz thimbles out. We choose the semiclassical ground state in the limit $\varepsilon \to +0$ as our initial condition. Since $\Psi' = e^{\text{Re}S/\varepsilon}\Psi$ and $\Psi^{(z_\sigma)} \to \delta(\mathcal{J}_\sigma)$ in $\varepsilon \to +0$, $\Psi'^{(z_\sigma)} \sim e^{\text{Re}S/\varepsilon}\delta(\mathcal{J}_\sigma)$ for small ε. Considering the Lefschetz thimble around z_0, for instance, its tangential direction at z_0 is given by $x_2 = \tan(\pi/8)x_1$, as also seen from Fig. 1. The initial wave function is thus proportional to

$$e^{\text{Re}S(z)/\varepsilon}\delta(-\sin(\pi/8)x_1 + \cos(\pi/8)x_2) \cdot (-\sin(\pi/8)dx_1 + \cos(\pi/8)dx_2). \tag{18}$$

The bosonic part is well localized at z_0, which justifies the following choice of the initial wave function, $\Psi'^{(z_\sigma)}(t = -\infty) = \delta(z - z_0)(-\sin(\pi/8)dx_1 + \cos(\pi/8)dx_2)$. Similarly, we can fix the initial wave function for $z_\pm$ as $\Psi'^{(z_\pm)} = \delta(z - z_\pm)(\cos(\pi/8)dx_1 + \sin(\pi/8)dx_2)$.

For the numerical procedure, we smear the delta function in the initial wave function by a Gaussian as $\delta(z - z_\sigma) \to \exp\{-20[(x_1 - x_{1\sigma})^2 + (x_2 - x_{2\sigma})^2]\}$. Then we discretize x_1 and x_2 from -2.5 to $+2.5$ with $dx = 5 \times 10^{-2}$. We then numerically integrate $\frac{d}{dt}\Psi'^{(z_\sigma)} = -H'_{\text{eff}}\Psi'^{(z_\sigma)}$ using the Euler method with $dt = 10^{-4}$ until the wave function converges. The convergence is fast and stable and the wave function hardly changes after $t = 1$–2. We also mention that we utilize the Crank–Nicolson algorithm to improve the numerical stability when we compute the Laplacian.

With this prescription, we find three independent ground-state wave functions $\Psi'^{(z_\sigma)} = \Psi_1'^{(z_\sigma)}dx_1 + \Psi_2'^{(z_\sigma)}dx_2$, shown in Fig. 2. Panels (a) and (b) in Fig. 2 show two components of $\Psi'^{(z_0)}$ and (c) and (d) show those of $\Psi'^{(z_+)}$. Since our system is symmetric under the reflection $z \mapsto -z$, we can easily read $\Psi'^{(z_-)}$ from the panels of $\Psi'^{(z_+)}$. Remarkably, these ground-state wave functions are linearly independent of each other, which means that supersymmetry is unbroken. We have also verified that the Dyson–Schwinger equation,

$$\lambda\left\langle z^4\right\rangle + \omega\left\langle z^2\right\rangle = 1, \tag{19}$$

is satisfied within 1% accuracy. This clearly shows that the supersymmetric quantum mechanics provides a suitable framework to compute Lefschetz thimbles.

Let us comment on the convergence of the wave functions in the present modified Lefschetz-thimble method. In the effective potential (16), the first term gives the dominant binding potential in our toy model for large $|z|$ because the first term is a polynomial up to the sixth order, while the second term is up to the quadratic order. Therefore, the convergence in the present numerical approach

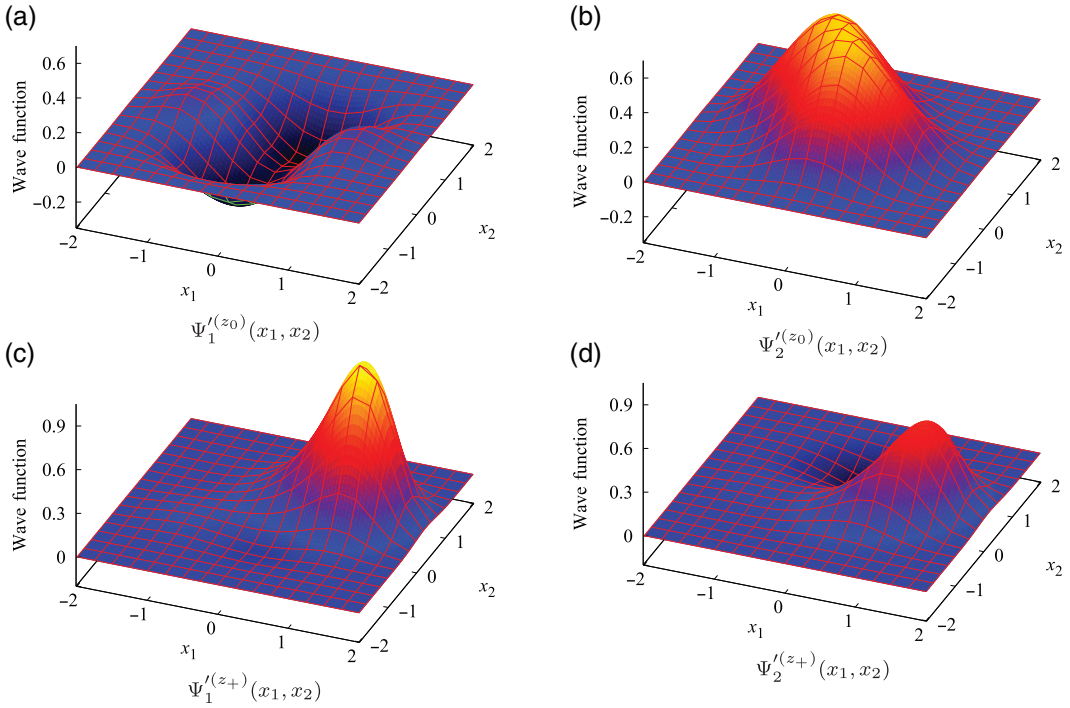

Fig. 2. SUSY ground state $\Psi'^{(z_\sigma)}$ corresponding to the saddle points $z_0 = 0$ and $z_+ = \sqrt{-\omega/\lambda}$ with $\varepsilon = 1$, $\omega = 1 - i$, and $\lambda = 10^{-3} + 1.5i$. Denoting $\Psi'^{(z_\sigma)} = \Psi_1'^{(z_\sigma)} dx_1 + \Psi_2'^{(z_\sigma)} dx_2$, (a) and (b) represent $\Psi'^{(z_0)}$, while (c) and (d) represent $\Psi'^{(z_+)}$.

is noticeably improved and there is no power-decay problem, unlike the complex Langevin method. One might think that the remaining $e^{i\mathrm{Im}S}$ is still oscillating, but this is not a problem in practice. We have numerically verified that the effect of $e^{i\mathrm{Im}S}$ is very small in the region where the profile of $\Psi'^{(z_\sigma)}$ is localized.

We also checked the robustness of the numerical results against small variations of the central position and the smearing width in the initial conditions. If the smearing width of the initial wave function is changed, the overall normalization would naturally also be changed, but, once we normalize the wave functions in the same manner (in Fig. 2 we normalized them as $\int dx_1\, dx_2 \left[\left(\Psi_1'^{(z_\sigma)}\right)^2 + \left(\Psi_2'^{(z_\sigma)}\right)^2\right] = 1$), then we eventually get the same result. Such insensitivity implies that each wave function is well localized and the overlap at the saddle point is small. However, the overlap at the saddle point is not completely zero. To see this effect, let us skew the relative weight of the initial conditions so that the initial wave functions are not orthogonal. In Fig. 3, we show $\tilde{\Psi}_1'^{(z_0)}$ and $\tilde{\Psi}_2'^{(z_0)}$ starting with the same relative weights, namely, $\tilde{\Psi}'^{(z_0)}(-\infty) = \delta(z - z_0)(dx_1 + dx_2)$ at the initial time, for demonstration purposes. The result $\tilde{\Psi}'^{(z_0)}$ in Fig. 3 is given a natural interpretation as a superposition of the three ground states shown in Fig. 2. Because of this overlap among wave functions, our prescription for the initial wave function needs further refinement in order to extract one Lefschetz thimble at $\varepsilon = 1$.

In order to see the importance of such refinements from another viewpoint, we checked the behaviors of distributions P for small ε. Setting $\varepsilon = 0.2$ with $\omega = 1 - i$ and $\lambda = 1.5i$, we obtain Figs. 4(a) and (b). Here, the normalization is given by $\int d^2x\, P = 1$. Although it is localized around the saddle point $z_0 = 0$, its shape is still far from the 1D line shown in Fig. 1. For comparison, we also show the result for $\varepsilon = 0.2$ with $\omega = 1 + i$ and $\lambda = 1.5i$ in Figs. 4(c) and (d). For this case, P is well localized

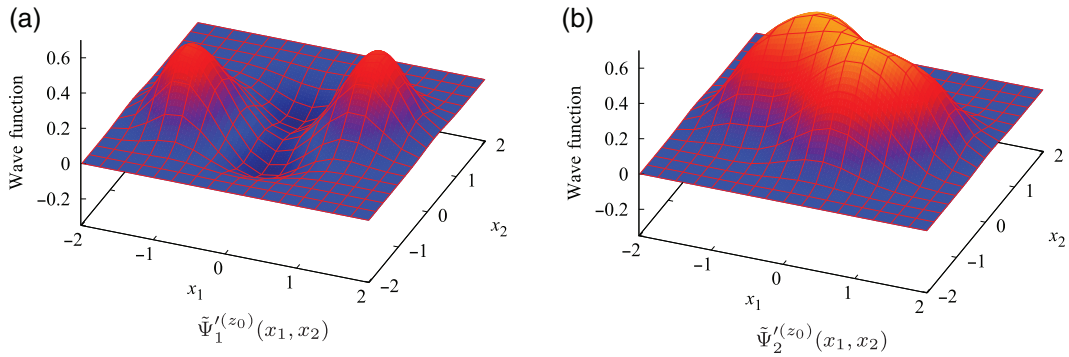

Fig. 3. SUSY ground state $\tilde{\Psi}'^{(z_0)}$, which is obtained starting with the saddle point z_0 but with the initial relative weight equal to both components.

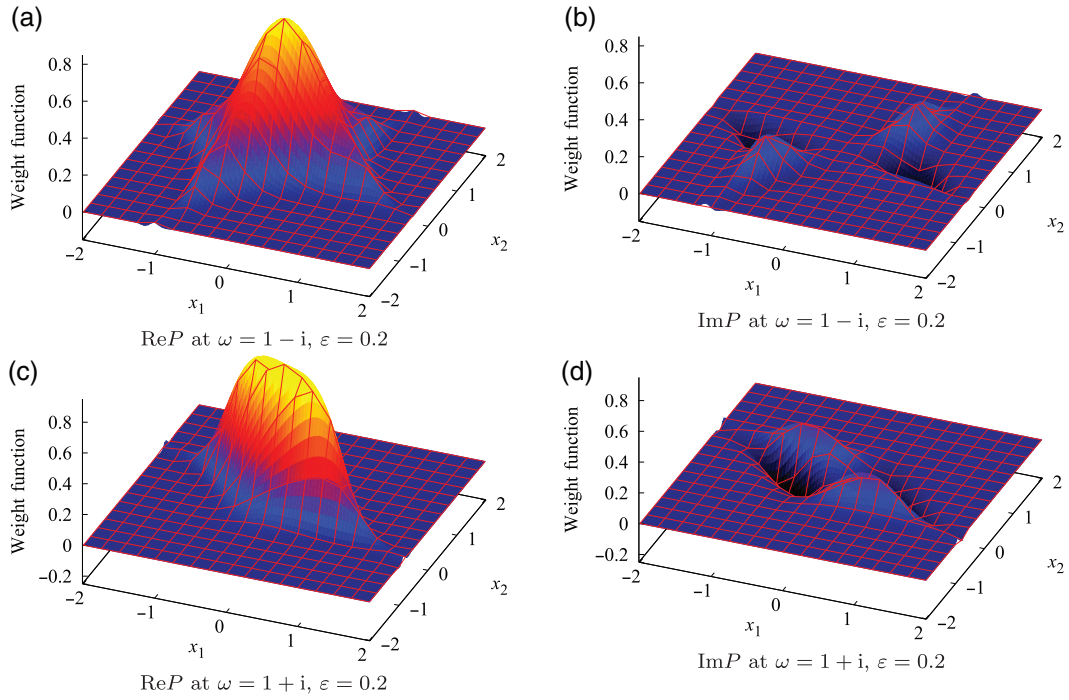

Fig. 4. Weight functions $P(x_1, x_2)$ corresponding to the saddle point z_0 with $\varepsilon = 0.2$. (a) and (b) show the result for $\omega = 1 - i$, and $\lambda = 10^{-3} + 1.5i$. (c) and (d) show the result for $\omega = 1 + i$, and $\lambda = 10^{-3} + 1.5i$.

to a 1D line, which is nothing but the Lefschetz thimble $\mathcal{J}_0$ at this parameter. We numerically observe that the weight function P is well localized around a Lefschetz thimble if Stokes phenomena do not occur and ε is sufficiently small. Expectation values of operators, such as $\langle z^2 \rangle$, also give correct numbers within the numerical accuracy with such parameters. However, as ε becomes larger, the wave functions spread as 2D distributions, and the expectation values of operators do not necessarily give correct values. Since the Dyson–Schwinger equation (19) is satisfied, this problem must come from superpositions of the wave function with other ground states.

An important future study would be to clarify the dependence on this initial condition more systematically, in order to take an appropriate linear combination of these wave functions giving each Lefschetz thimble. This would be a key step in studying how the Stokes phenomenon is realized at $\varepsilon = 1$. It would also open a new possibility to take into account multiple Lefschetz thimbles, since ground-state wave functions can be superposed by changing the initial conditions.

5. *Discussions and conclusions* In this letter, the supersymmetric reformulation of the Lefschetz-thimble integration was studied and its practical computation was discussed. Lefschetz thimbles are now regarded as the ground states of a supersymmetric Hamiltonian. Our computational scheme for the Hamiltonian system is essentially the same as that for the Fokker–Planck equation in the complex Langevin method. These supersymmetric wave functions are numerically computed for a 0D toy model with the classical action $S = S_0 + S_{\rm int}$, where $S_0 = -\frac{\omega}{2}x^2$ and $S_{\rm int} = -\frac{\lambda}{4}x^4$. Since the Morse indices of all the saddle points are the same, the number of saddle points must be the same as that of linearly independent ground states.

For the Gaussian model with S_0 only, the above-mentioned situation is clearly true; this is explicitly checked by computing the wave function analytically and constructing one supersymmetric ground state. From this almost trivial example, one can learn an important lesson about the 2D smooth distribution $P_0(z, \bar{z})$. In the "semiclassical" limit of $\varepsilon \to 0$, we recover a delta-functional support along the Lefschetz thimble in the original formulation. For nonzero ε, the phase oscillation arises away from the Lefschetz thimble, and the formulation nevertheless reproduces the correct expectation value.

For the interacting model with $S_{\rm int}$, we performed numerical computations for the supersymmetric quantum mechanics, and confirmed the existence of three linearly independent ground states by restricting ourselves to the $F = 1$ sector. Since the wave function in the $F = 1$ sector consists of two components, we must set them in the proper initial conditions. We started from a localized wave function in the vicinity of each saddle point, and our numerical computation shows remarkable stability under small modifications of the initial conditions. This reflects the fact that all the saddle points are attractive, unlike the complex Langevin method. At the same time, we also found substantial dependence on the initial relative weight of these two components. This clearly indicates that we need a careful refinement of the initial conditions to use the modified Lefschetz-thimble method for numerical simulations, but it also opens a new possibility for some convenient scheme to take into account multiple Lefschetz thimbles.

In the case of the Fokker–Planck system, the ground state is often uniquely determined and the initial-condition dependence does not appear, as in the case in ordinary quantum mechanics without any special symmetry. The Fokker–Planck operator of the complex Langevin method can be written as a functional integral in a similar manner, and it also shows the same type of BRST symmetry. There are, however, several important differences between these two formalisms: First of all, the diffusion term in the complex Langevin equation does not give the gradient flow because the sign is different. Because of this difference, the BRST invariance cannot be promoted to the supersymmetric system satisfying $2H = \{Q, \bar{Q}\}$ with supercharges Q, $\bar{Q}$. Moreover, the fermionic sector should be restricted to $F = 2$ instead of $F = 1$. Therefore, it is not straightforward to relate these two formalisms yet. If one could establish a firm relationship between the two methods, it would be great progress and the present modified Lefschetz thimble could provide us with an opportunity for a fully complementary approach to the sign problem together with the complex Langevin method.

Acknowledgements

The authors thank Yuya Abe, So Matsuura, Jun Nishimura, and Jan Pawlowski for useful discussions. K.F. was supported by JSPS KAKENHI Grant Nos. 15H03652 and 15K13479. Y.T. was supported by Grants-in-Aid for JSPS fellows (No. 25-6615). This work was partially supported by the RIKEN iTHES project, and also by the Program for Leading Graduate Schools, MEXT, Japan.

Funding

Open Access funding: SCOAP.[3]

References

[1] E. Y. Loh, J. E. Gubernatis, R. T. Scalettar, S. R. White, D. J. Scalapino, and R. L. Sugar, Phys. Rev. B **41**, 9301 (1990).
[2] S. Muroya, A. Nakamura, C. Nonaka, and T. Takaishi, Prog. Theor. Phys. **110**, 615 (2003) [arXiv:hep-lat/0306031] [Search INSPIRE].
[3] F. Pham, Proc. Symp. Pure Math. Vol. 40.2, pp. 319–333 (1983).
[4] E. Witten, Analytic continuation of Chern–Simons theory, in *Chern–Simons Gauge Theory: 20 Years After*, eds. J. E. Andersen, H. U. Boden, A. Hahn, and B. Himpel (American Mathematical Society and International Press of Boston, Inc., 2010), Vol. 50, pp. 347–446 [arXiv:1001.2933 [hep-th]] [Search INSPIRE].
[5] E. Witten, [arXiv:1009.6032 [hep-th]] [Search INSPIRE].
[6] M. Cristoforetti, F. Di Renzo, and L. Scorzato, Phys. Rev. D **86**, 074506 (2012) [arXiv:1205.3996 [hep-lat]] [Search INSPIRE].
[7] M. Cristoforetti, F. Di Renzo, A. Mukherjee, and L. Scorzato, Phys. Rev. D **88**, 051501 (2013) [arXiv:1303.7204 [hep-lat]] [Search INSPIRE]
[8] H. Fujii, D. Honda, M. Kato, Y. Kikukawa, S. Komatsu, and T. Sano, J. High Energy Phys. **1310**, 147 (2013) [arXiv:1309.4371 [hep-lat]] [Search INSPIRE].
[9] M. Cristoforetti, F. Di Renzo, G. Eruzzi, A. Mukherjee, C. Schmidt, L. Scorzato, and C. Torrero, Phys. Rev. D **89**, 114505 (2014) [arXiv:1403.5637 [hep-lat]] [Search INSPIRE].
[10] Y. Tanizaki and T. Koike, Ann. Phys. **351**, 250 (2014) [arXiv:1406.2386 [math-ph]] [Search INSPIRE].
[11] Y. Tanizaki, Phys. Rev. D **91**, 036002 (2015) [arXiv:1412.1891 [hep-th]] [Search INSPIRE].
[12] T. Kanazawa and Y. Tanizaki, J. High Energy Phys. **1503**, 044 (2015) [arXiv:1412.2802 [hep-th]] [Search INSPIRE].
[13] Y. Tanizaki, H. Nishimura, and K. Kashiwa, Phys. Rev. D **91**, 101701 (2015) [arXiv:1504.02979 [hep-th]] [Search INSPIRE].
[14] F. Di Renzo and G. Eruzzi, [arXiv:1507.03858 [hep-lat]] [Search INSPIRE].
[15] P. H. Damgaard and H. Huffel, Phys. Rept. **152**, 227 (1987).
[16] G. Aarts and F. A. James, J. High Energy Phys. **08**, 020 (2010) [arXiv:1005.3468 [hep-lat]] [Search INSPIRE].
[17] H. Makino, H. Suzuki, and D. Takeda, [arXiv:1503.00417 [hep-lat]] [Search INSPIRE].
[18] J. Nishimura and S. Shimasaki, Phys. Rev. D **92**, 011501 (2015) [arXiv:1504.08359 [hep-lat]] [Search INSPIRE].
[19] J. Berges and I. O. Stamatescu, Phys. Rev. Lett. **95**, 202003 (2005) [arXiv:hep-lat/0508030] [Search INSPIRE].
[20] J. Berges, Sz. Borsanyi, D. Sexty, and I. O. Stamatescu, Phys. Rev. D **75**, 045007 (2007) [arXiv:hep-lat/0609058] [Search INSPIRE].
[21] R. Anzaki, K. Fukushima, Y. Hidaka, and T. Oka, Ann. Phys. **353**, 107 (2015) [arXiv:1405.3154 [hep-ph]] [Search INSPIRE].
[22] E. Frenkel, A. Losev, and N. Nekrasov, Nucl. Phys. Proc. Suppl. **171**, 215 (2007) [arXiv:hep-th/0702137] [Search INSPIRE].
[23] E. Frenkel, A. Losev, and N. Nekrasov, [arXiv:hep-th/0610149] [Search INSPIRE].
[24] E. Frenkel, A. Losev, and N. Nekrasov, [arXiv:0803.3302 [hep-th]] [Search INSPIRE].
[25] E. Witten, J. Diff. Geom. **17**, 661 (1982).
[26] A. Behtash, E. Poppitz, T. Sulejmanpasic, and M. Ünsal, [arXiv:1507.04063 [hep-th]] [Search INSPIRE].
[27] G. Aarts, Phys. Rev. D **88**, 094501 (2013) [arXiv:1308.4811 [hep-lat]] [Search INSPIRE].
[28] G. Aarts, L. Bongiovanni, E. Seiler, and D. Sexty, J. High Energy Phys. **1410**, 159 (2014) [arXiv:1407.2090 [hep-lat]] [Search INSPIRE].